Cerebral Cortex Advance Access published July 17, 2014

Cerebral Cortex
doi:10.1093/cercor/bhu156

Satb2 Regulates the Differentiation of Both Callosal and Subcerebral Projection Neurons in the Developing Cerebral Cortex

Dino P. Leone[1], Whitney E. Heavner[1], Emily A. Ferenczi[2], Gergana Dobreva[3], John R. Huguenard[2], Rudolf Grosschedl[3] and Susan K. McConnell[1]

[1]Department of Biology, Stanford University, Stanford, CA 94305, USA, [2]Department of Neurology and Neurological Sciences, Stanford University School of Medicine, Stanford, CA 94305, USA and [3]Max Planck Institute of Immunobiology and Epigenetics, Freiburg 79108, Germany

Address Correspondence to Email: suemcc@stanford.edu

The chromatin-remodeling protein Satb2 plays a role in the generation of distinct subtypes of neocortical pyramidal neurons. Previous studies have shown that *Satb2* is required for normal development of callosal projection neurons (CPNs), which fail to extend axons callosally in the absence of *Satb2* and instead project subcortically. Here we conditionally delete *Satb2* from the developing neocortex and find that neurons in the upper layers adopt some electrophysiological properties characteristic of deep layer neurons, but projections from the superficial layers do not contribute to the aberrant subcortical projections seen in *Satb2* mutants. Instead, axons from deep layer CPNs descend subcortically in the absence of *Satb2*. These data demonstrate distinct developmental roles of *Satb2* in regulating the fates of upper and deep layer neurons. Unexpectedly, *Satb2* mutant brains also display changes in gene expression by subcerebral projection neurons (SCPNs), accompanied by a failure of corticospinal tract (CST) formation. Altering the timing of *Satb2* ablation reveals that SCPNs require an early expression of *Satb2* for differentiation and extension of the CST, suggesting that early transient expression of Satb2 in these cells plays an essential role in development. Collectively these data show that *Satb2* is required by both CPNs and SCPNs for proper differentiation and axon pathfinding.

Keywords: callosal projection neuron, corticospinal tract, Ctip2, development, Fezf2, pyramidal neuron, specification

Introduction

While the mammalian cerebral cortex contains a multitude of distinct cell types, neurons can be broadly classified into 2 major groups: excitatory glutamatergic projection neurons and GABAergic inhibitory interneurons. The projection neurons can, in turn, be subdivided into 3 major subclasses (reviewed in Leone et al. 2008; Greig et al. 2013): corticofugal projection neurons, commissural projection neurons, and ipsilateral local circuit connection neurons (associative projection neurons). Corticofugal projection neurons (also called subcortical projection neurons) are located in the deep Layers 5 and 6 and send their axons to subcortical targets such as the thalamus and subcerebral targets such as the midbrain and spinal cord (subcerebral projection neurons, SCPNs). Commissural projection neurons send interhemispheric axons across the midline either along the corpus callosum (callosal projection neurons; CPNs; reviewed in Fame et al. 2011), or through the anterior commissure. The majority of CPNs are found in superficial layers, but they also populate the deep Layers 5 and 6.

The production of these distinct subtypes requires a number of key transcription factors including *Fezf2* (also known as *Fezl* or *Zfp312*), which regulates the specification of SCPNs (Molyneaux et al. 2005; Chen et al. 2005, 2008; Shim et al. 2012), *Ctip2* (also known as *Bcl11b*), which is necessary for axonal outgrowth of SCPNs (Arlotta et al. 2005), *Tbr1*, which is required for Layer 6 corticothalamic neurons (Hevner et al. 2001; Han et al. 2011; McKenna et al. 2011), and *Satb2*, which is essential for the specification of CPNs (Alcamo et al. 2008; Britanova et al. 2008; Zhang et al. 2012). These factors interact with additional transcription factors that further refine fate acquisition. For example, *Sox5* controls the timing of corticofugal neuron generation (Lai et al. 2008) and is also required postmitotically for the repression of *Fezf2,* ultimately regulating the generation of distinct subtype identities in Layers 5, 6, and the subplate (Kwan et al. 2008). In addition, the transcription factor *Bhlhb5* is required during the postmitotic acquisition of area identity and differentiation of SCPNs (Joshi et al. 2008). Taken together, these data suggest that initial specification of pyramidal neurons occurs in early postmitotic, immature neurons, but definitive fates are achieved during differentiation.

The chromatin-remodeling protein Satb2 was first identified as a matrix attachment region (MAR)-binding protein (Dobreva et al. 2003), and we and others subsequently showed that *Satb2* is a major regulator of CPNs in the developing cerebral cortex (Alcamo et al. 2008; Britanova et al. 2008). The axons of *Satb2*-deficient pyramidal neurons fail to cross the corpus callosum and instead project subcortically. In *Satb2* mutants, expression of *Ctip2*, a transcription factor normally expressed by Layer 5 neurons (Arlotta et al. 2005; Molyneaux et al. 2005), is expanded into the superficial layers, suggesting that CPNs in the absence of *Satb2* adopt characteristics of subcortical projection neurons. Biochemical studies revealed that Satb2 binds to regulatory regions (MAR sequences) in the *Ctip2* locus and thereby represses *Ctip2* expression directly (Alcamo et al. 2008). However, effective repression of *Ctip2* requires the protooncogene Ski, which is necessary for the formation of a multi-protein complex consisting of Ski, Satb2, and the histone deacetylases HDAC1 and MTA2 that enables Satb2 to act as a repressor (Baranek et al. 2012).

The fates of cortical projection neurons are defined by a large number of factors besides their long-distance projections, since cells in different layers develop distinct electrophysiological signatures, local axonal connections, dendritic morphologies, and patterns of gene expression (reviewed in Molyneaux et al. 2007; Leone et al. 2008; Greig et al. 2013). In our previous studies, we were unable to examine many of these features that emerge postnatally, since mice bearing a null mutation in *Satb2* die at birth. Here we analyze conditional *Satb2* mice using different Cre driver lines that allowed us to bypass the

early lethality of a null mutation and to ablate *Satb2* at different time points during development. These studies reveal distinct roles of *Satb2* in regulating the electrophysiological characteristics of upper layer neurons and the long-distance connections of CPNs in the upper versus deep layers. In addition, we have discovered an unexpected role for *Satb2* in the differentiation of *Fezf2*-expressing SCPNs and the corticospinal tract (CST).

Materials and Methods

Animals

Conditional mutants were generated by breeding Emx1-Cre;Satb2$^{+/lacZ}$, Rbp4-Cre;Satb2$^{+/lacZ}$ or Nestin-Cre^{ERT2};Satb2$^{+/lacZ}$ mice with Satb2$^{lox/lox}$ animals to obtain mutant (Cre^{+};Satb2$^{lox/lacZ}$) and control (Cre^{+};Satb2$^{+/lox}$) littermates. For some experiments, Cre^{+};Satb2$^{+/lacZ}$ controls were used. Finally, for some experiments, animals were also heterozygous for the Fezf2^{AP} allele (Chen et al. 2005) or the reporter allele Ai9 (Madisen et al. 2010). See Supplementary Methods for genotyping. The morning of the vaginal plug was defined as E0.5. For Nestin-Cre^{ERT2} experiments, pregnant females were injected with a single dose of 0.2–0.3 mg Tamoxifen (Sigma) dissolved in Dimethyl sulfoxide (Sigma).

Histology, Immunocytochemistry, Antibodies, and In Situ Hybridization

Standard protocols for immunohistochemistry were used. Perinatal animals were perfused on postnatal day P4 with 4% paraformaldehyde (PFA) supplemented with 0.1% saponin in Dulbecco's phosphate buffered saline (PBS), and all other postnatal animals were perfused with 4% paraformaldehyde in PBS. Embryonic brains were dissected and drop-fixed in 4% paraformaldehyde at least overnight. Brains were cryoprotected in 30% sucrose in PBS and either embedded in OCT tissue tek for cryosectioning (20 µm) or directly cut on a sliding microtome (70 µm). Radioactive in situ hybridization was carried out as previously described (Frantz et al. 1994); see Supplementary Methods for list of probes.

We used the following primary antibodies: rabbit anti-Satb2 (Abcam), mouse anti-Satb2 (Abcam), rat anti-Ctip2 (Abcam), rabbit anti-red fluorescent protein (RFP) (Clontech), rabbit anti-protein kinase Cγ (PKCγ) (Santa Cruz Biotechnology), chicken anti-β-galactosidase (Abcam), rabbit anti-Tbr1 (Abcam), rabbit anti-Fog2 (Abcam), and rat anti-L1 (Millipore). Alexa Fluor-coupled secondary antibodies were used to detect primary antibodies.

For alkaline phosphatase (AP) staining, fixed brains were incubated in PBS at 65°C for 25 min to inactivate endogenous phosphatases, stained with NBT/BCIP (Roche) in 100 mM Tris–HCl, 50 mM $MgCl_2$, pH 9.5 at 37°C and postfixed with PFA. For X-gal histochemistry, brains were fixed in 2% formaldehyde/0.2% glutaraldehyde in PBS for 10 min., stained with 1 mg/mL X-gal for ~2 h, and postfixed with PFA.

Confocal images were acquired on a Zeiss LSM 510 meta microscope, and epifluorescent pictures were taken on a Nikon 80i with a Hamamatsu Orca ER camera. Images were postprocessed using Adobe Photoshop CS3 and ImageJ.

Retrograde Tracing

For retrograde tracing, P15 animals were anesthetized with ketamine and xylazine and their heads were stabilized in a stereotaxic frame. The brain was exposed and 0.1 µL of fluorescent labeled latex beads (Lumafluor Inc.) were injected into either the thalamus, the anterior pretectal nucleus, or the cerebral peduncle using a stereotaxic injector (Stoelting). Animals were sacrificed 48–60 h after surgery to allow for transport of the beads.

Anterograde Tracing

Anterograde tracings were performed according to instructions (Vector Laboratories; Gerfen and Sawchenko 1984). Briefly, P15 animals were anesthetized and PHA-L was infused using glass capillaries with an interior diameter of 15 µm. Iontophoresis was performed using 5 µA pulses for 10–15 min using 7 s intervals (7 s current, 7 s pause). After allowing 48 h for PHA-L transport, animals were perfused and processed using the Vectastain ABC kit (Vector Laboratories).

Electrophysiology

Acute coronal slices (300 µm) were prepared from P21–P25 mutant and control littermates. Slices were incubated at 37°C for 1 h in artificial cerebrospinal fluid (ACSF) containing 126 mM NaCl, 2.5 mM KCl, 1.25 mM NaH_2PO_4, 26 mM $NaHCO_3$, 1 mM $MgSO_4{\cdot}7H_2O$, 2 mM $CaCl_2{\cdot}H_2O$, and 10 mM glucose, equilibrated with 95% O_2 and 5% CO_2 prior to being transferred to a submerged recording chamber perfused with warmed (30–34°C), oxygenated ACSF at 1–2 mL/min. Whole-cell patch-clamp recordings in current-clamp mode were made from superficial layer pyramidal neurons in presence of synaptic blockers (50 µM picrotoxin and 1 mM kynurenic acid). Recording electrodes made of borosilicate glass were pulled to a final tip resistance of 3–6 MΩ and filled with internal solution as per Chen et al. (2008). Intracellular recordings and analysis were performed using pClamp (Molecular Devices). Mean resting membrane potentials were −71.9 and −75.4 mV for mutants and controls, respectively, and input resistance were 178 and 133 MΩ for mutants and controls, respectively, not significantly different between the 2 groups ($n = 17$ and 19 for mutant and control group, respectively).

Results

Altered Projections in Satb2-deficient Mice

A *lacZ* gene inserted into the *Satb2* null allele (Supplementary Fig. 1) previously allowed us to visualize changes in the projections of *Satb2*-expressing neurons (Alcamo et al. 2008; Srinivasan et al. 2012), but perinatal lethality precluded a detailed postnatal analysis of these tracts. To circumvent early lethality, we employed a conditional *Satb2* allele (Satb2^{lox}, Supplementary Fig. 1) in tandem with the Emx1-Cre driver line, which limits recombination to dorsal neocortex (Gorski et al. 2002). We assessed the efficiency of recombination by using the Ai9 reporter allele (Madisen et al. 2010), in which a CAG-driven RFP cDNA, preceded by a floxed-stop cassette, is inserted into the Rosa26 locus (Soriano 1999), leading to RFP expression in recombined cells. The Ai9 reporter construct carries at its 3′ end a woodchuck hepatitis virus post-transcriptional regulatory element that enhances mRNA stability (Madisen et al. 2010), enabling visualization of axons and dendritic arbors in RFP^{+} neurons. Emx1-Cre conferred efficient recombination of both the Satb2^{lox} (Fig. 1) and Ai9 reporter alleles. In control *Emx1-Cre;Satb2$^{lox/+}$;Ai9* mice at P4, Satb2 protein was readily detected in neocortex (Fig. 1*A*), and the vast majority of Satb2^{+} neurons in both superficial (Fig. 1*C*,*C*′) and deep layers (Fig. 1*E*) colabeled with RFP. In *Emx1-Cre;Satb2* mutants, Satb2 expression was lost in all layers (Fig. 1*B*,*D*,*D*′,*F*), suggesting a high recombination efficiency for Emx1-Cre. Conditional mutant mice survived the juvenile period, but died between P25–30 for unknown reasons. In both null and conditional mutants, Satb2-expressing neurons and their axons are marked by β-galactosidase expression.

In previous studies of *Satb2*$^{-/-}$ mice, the axons of CPNs failed to extend across the corpus callosum and instead formed aberrant subcortical projections; in addition, the deep layer markers Ctip2, Ldb2, Grb14, and Kitl were upregulated in superficial layer neurons, suggesting that the fates of these cells had been altered (Alcamo et al. 2008; Britanova et al. 2008). Conditional mutants recapitulate many but not all of these phenotypes. Interestingly, whereas *Satb2*$^{-/-}$ mice at E18.5 lacked labeled axons in the corpus callosum (Alcamo

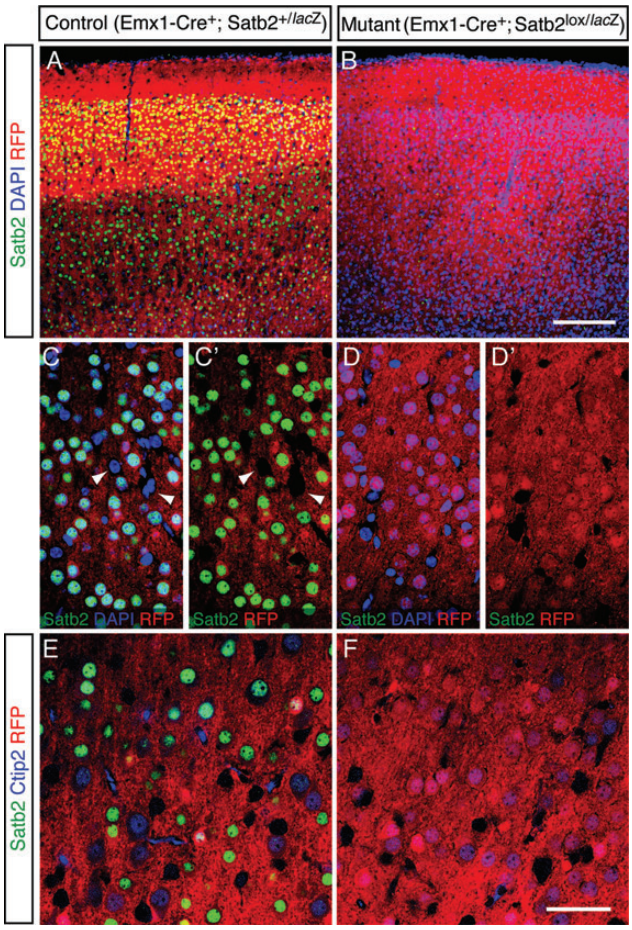

Figure 1. *Emx1-Cre* efficiently ablates *Satb2* in neocortical pyramidal neurons. Coronal sections of P4 neocortex were assessed for Cre recombination efficiency. Animals carried the *Ai9* RFP reporter allele to mark cells that have undergone recombination. Satb2 (green, *A–F*) is readily observed in *Emx1-Cre*$^{+}$*;Satb2*$^{+/lacZ}$*;Ai9*$^{+}$ (control) neocortex in Layers 2–6 (*A*), but completely lost in *Emx1-Cre*$^{+}$*;Satb2*$^{lox/lacZ}$*;Ai9*$^{+}$ (mutants; *B*). (*C*, *C'*) High power confocal pictures of the superficial layers of control animals show that the vast majority of Satb2^{+} neurons coexpress RFP, which, due to its high mRNA stability is detected almost ubiquitously except for nuclei. Note that RFP^{-} cells (blue in *C*; arrowheads in *C* and *C'*) do not express Satb2, suggesting that these non-recombined cells are either interneurons or endothelial cells. (*D*, *D'*) High power confocal pictures of superficial layers of a mutant shows complete loss of Satb2. (*E*, *F*) High power confocal pictures of Layer 5 in control (*E*) and mutant (*F*) neocortex shows loss of Satb2 in the deep layers of mutants. Scale bars: 200 μm in *B* for *A*, *B*; 50 μm in *F* for *C–F*.

et al. 2008), examination of postnatal *Emx1-Cre;Satb2* mutants revealed some β-galactosidase^{+} axons in the corpus callosum and others following an aberrant pathway into the septum (Supplementary Fig. 2*B*). It is conceivable that Satb2 is required for early-born pioneer axons to cross the corpus callosum, but that some axons at later stages can reach the contralateral hemisphere in the absence of *Satb2*. Consistent with this possibility, the expression of *Crystallin μ* (*CRYM*) expanded into the superficial layers in cingulate cortex (Fig. 2*B*), which contains neurons that pioneer the corpus callosum (Koester and O'Leary 1994; Rash and Richards 2001; Fothergill et al. 2013). This region normally expresses the zinc-finger protein Fog-2 (also known as Zfpm2; Fig. 2*C*), but in *Emx1-Cre;Satb2* mutants, *Fog-2* expression in superficial layers of cingulate cortex is abrogated (Fig. 2*D*). These changes may relate to the failure of callosal development in *Satb2* null mutants at E18.5 and a defect in the ability of the cingulate pioneers and early-generated neurons to extend callosal axons. In the neocortex, *CRYM* expression, which is normally present in differentiating SCPNs (Fig. 2*A*,*A'*; Arlotta et al. 2005), was markedly expanded across the entire cerebral wall in *Emx1-Cre;Satb2* mutants (Fig. 2*B*,*B'*), adding to the list of deep layer markers that are upregulated in upper layer neurons in the absence of *Satb2*. The SCPN markers *Diap3* and *Crim1* showed no obvious changes in conditional mutants (data not shown).

Consistent with previous reports, control animals showed no β-galactosidase labeling of subcortical axon tracts in the thalamus or cerebral peduncle, although weak β-galactosidase activity was present in the internal capsule (Supplementary Fig. 2C) likely resulting from callosal neurons that extend collateral axons to the striatum (Mitchell and Macklis 2005; reviewed in Fame et al. 2011). Both null and conditional mutants showed a dramatic increase in β-galactosidase^{+} axons extending subcortically within the internal capsule (Supplementary Fig. 2B), thalamus and cerebral peduncle (Supplementary Fig. 2D). In postnatal *Emx1-Cre;Satb2* mutants we also observed β-galactosidase^{+} axons within the CST (Supplementary Fig. 2F), providing new evidence that the identity of at least some *Satb2*-expressing neurons is altered toward a SCPN fate in *Satb2* mutants. However, these studies do not address whether the β-galactosidase^{+} CST axons arise from upper layer neurons or from the smaller population of Satb2^{+} cells that reside in the deep layers.

Superficial layer neurons in Satb2 mutants adopt some electrophysiological properties that are characteristic of deep layer neurons.

To further assess whether upper layer neurons adopt characteristics typical of deep layer cells in the absence of *Satb2*, we examined their electrophysiological properties. Normal Layer 5 SCPNs fire distinct bursts with fixed, short interspike intervals in response to a current injection (Kasper et al. 1994), and are characterized by voltage responses that include an early peak and then decay, the so-called sag response (Stafstrom et al. 1984). Superficial layer CPNs, on the other hand, have been described as non-bursting (Larkman and Mason 1990; Mason and Larkman 1990; Kasper et al. 1994) and they lack a voltage sag response.

To investigate whether changes in gene expression by upper layer neurons in *Satb2* mutants correlate with changes in layer-specific electrophysiological properties, we recorded from superficial layers of *Emx1-Cre;Satb2* mutants and littermate controls. Acute coronal slices were prepared from P25 animals and whole-cell patch-clamp recordings in current-clamp mode were made from Layer 2/3 pyramidal neurons in primary somatosensory cortex. We did not detect significant differences in action potential threshold, firing frequency, burst firing or adaptation ratio between mutant and control neurons (Supplementary Table 1). We did, however, detect differences in these cells' responses to injection of a 100 pA hyperpolarizing current step, and representative voltage responses from a control and mutant neuron are shown in Figure 3*A*. *Emx1-Cre;Satb2* mutant neurons showed a significantly increased sag response (which immediately follows current injection; Fig. 3*A*,*C*) and a doubling of the after-depolarization in response to current injection (Fig. 3*A*,*C*). Full families of voltage responses to current steps

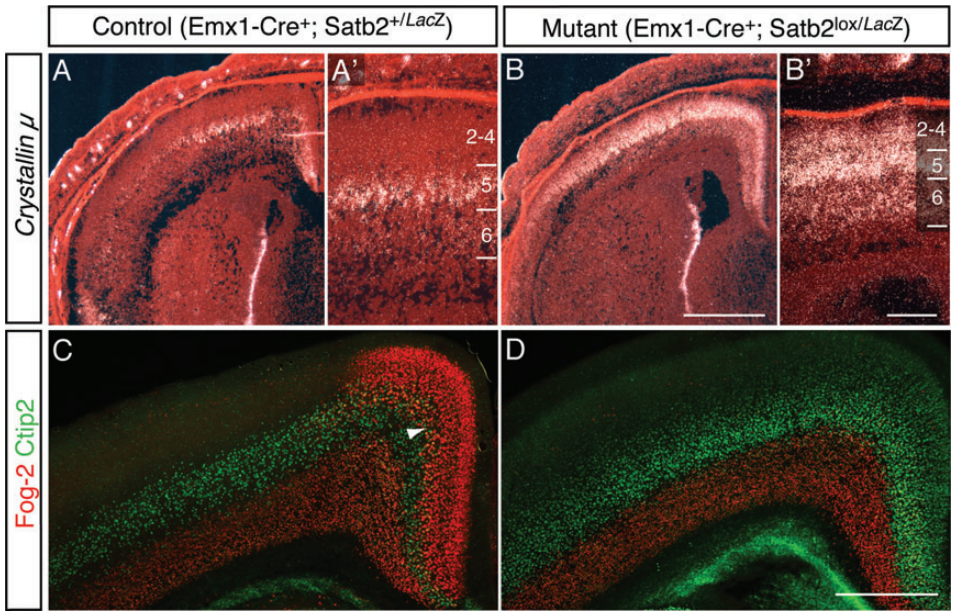

Figure 2. Molecular changes in superficial layers of *Emx1-Cre;Satb2* mutant mice. *In situ* hybridization on coronal P1 sections. (*A–B′*) *Crystallin μ* (*CRYM*), a SCPN marker, is expressed by Layer 5 neurons of *Emx1-Cre*$^{+}$*;Satb2*$^{+/LacZ}$ (controls; *A*, *A′*), but is strikingly upregulated across the entire cortical wall of *Emx1-Cre*$^{+}$*;Satb2*$^{lox/lacZ}$ (mutants; *B*, *B′*). (*C–D*) Immunohistochemistry for Fog-2 (red in *C*, *D*) and Ctip2 (green in *C*, *D*) on coronal sections of P4 brains shows strong expression of Fog-2 in Layer 6 and the superficial layers of cingulate cortex in controls (arrowhead in *C*), but a loss of Fog-2 expression in mutant cingulate cortex (*D*). Scale bars: 1 mm in *B* for *A*, *B*; 100 μm in *B′* for *A′*, *B′*, 500 μm in *D* for *C*, *D*.

from −100 to +100 pA are shown in Supplementary Figure 3. Quantification revealed statistically significant increases in both the sag response (mutants: 2.17 ± 0.39 mV; controls: 0.42 ± 0.1 mV; $P < 0.01$) and after depolarization (mutants: 2.06 ± 0.30 mV; controls: 0.75 ± 0.16 mV; $P < 0.01$).

The dramatic increase in sag response in *Emx1-Cre;Satb2* mutants (Fig. 3*C*) suggests a prominent hyperpolarization-activated current I_h, an inward, excitatory current that is normally high in SCPNs, where it plays important roles in rhythmic firing (resonance) and production of sag currents; I_h is low in corticostriatal and corticocortical projection neurons (Dembrow et al. 2010; Sheets et al. 2011). Analysis of peak versus end-of-pulse voltage responses in *Satb2* mutants and controls (Fig. 3*B*) revealed a statistically significant interaction (2-way analysis of variance [ANOVA]; $F_{1,25} = 13.12$, $P = 0.0013$) after correction for multiple comparisons (Holm–Sidak method). I_h currents are mediated by hyperpolarization-activated cyclic nucleotide-gated (HCN) cation channels, which are encoded by the *HCN1–4* gene family. In a microarray screen for genes that showed differential expression in the *Satb2*$^{-/-}$ mutant cortex, we found that *HCN1* is upregulated 3.8-fold in *Satb2* mutants compared with controls (data not shown). To validate the array findings, we performed in situ hybridization for *HCN1* at E18.5. In control mice, *HCN1* is expressed at high levels in the deep layers (Fig. 3*D*), in agreement with previous reports (Nolan et al. 2003; Sheets et al. 2011; Stoenica et al. 2013). However, in *Satb2*$^{-/-}$ mutants, *HCN1* expression was elevated in the superficial layers (as well as in Layer 6; Fig. 3*E*). Surprisingly, we measured a statistically significantly higher membrane resistance in *Emx1-Cre;Satb2* mutants compared with controls (0.178 ± 0.014 GΩ vs. 0.133 ± 0.016 GΩ; Supplementary Table 1). The mechanism for the increased input resistance remains unknown, but did not affect our ability to detect the sag response induced by current injections that produced similar levels of hyperpolarization. Taken together, our data show that *Satb2*-deficient superficial layer neurons display a strong sag response, a high I_h current and a striking increase in *HCN1* expression, all of which are normally characteristic of Layer 5 SCPNs.

Aberrant Subcortical Projections in Satb2 Mutants Arise Exclusively From the Deep Layers

The anatomical, electrophysiological, and molecular changes observed in *Emx1-Cre;Satb2* mutants raise the possibility that superficial layer neurons contribute to the aberrant extension of subcortical projections by β-galactosidase^{+} axons. To address this hypothesis, we performed a more detailed analysis of subcortical projections and their laminar origins in mutant and control animals.

We first examined corticothalamic projections, which can be visualized using the *golli*-τ-GFP transgene (*golli*-GFP; Jacobs et al. 2007) in which 1.3 kb of the *golli* promotor of the myelin basic protein gene directs the expression of a τ-EGFP cassette to deep layer pyramidal neurons, including Layer 6 corticothalamic neurons (Supplementary Fig. 4) and CPNs in Layers 5 and 6 that project across the corpus callosum (data not shown). In sagittal sections of P4 control animals expressing *golli*-GFP, robust GFP expression marked Layers 5 and 6 (Supplementary Fig. 4A) as well as axons in the internal capsule and thalamus (Supplementary Fig. 4A), as expected. In *Emx1-Cre;Satb2* mutant brains, *golli*-GFP reactivity remained confined to the deep layers, although it appears increased in Layer 6 (Supplementary Fig. 4B). While thalamic GFP expression appeared similar to controls, axonal GFP^{+} staining in the mutant internal capsule (Supplementary Fig. 4B) appeared more prominent. The failure of upper layer neurons to acquire *golli*-GFP expression, together with enhanced staining of axons in the internal capsule, raised an alternative to the hypothesis that upper layer neurons redirect their axons in *Satb2* mutants. These

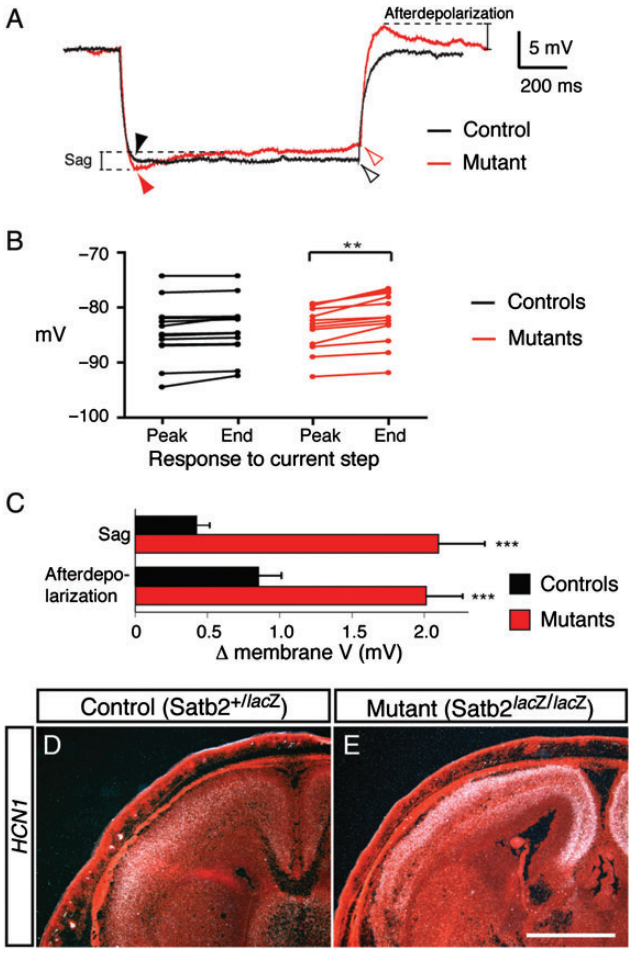

Figure 3. *Satb2*-deficient superficial layer neurons adopt some electrophysiological characteristics of deep layer neurons. (*A–C*) Layer 2/3 neurons of somatosensory cortex were whole-cell patch-clamped in current-clamp mode and recorded in acute cortical slices prepared from P25 mutant and control animals. *Satb2* mutant upper layer neurons acquired a hyperpolarization-activated current in response to a 100 pA current step. (*A*) Overlay of representative responses of patch-clamped neurons from Layer 2/3 control (*Emx1-Cre*$^{+}$*;Satb2*$^{+/LacZ}$; black) and mutant animal (*Emx1-Cre*$^{+}$*; Satb2*$^{lox/LacZ}$; red). Peak of responses (arrowheads) and end-of-step (open arrowheads) show differences in sag responses for mutants (red) and controls (black). (*B*) Quantification of voltage differences between the peak and end-of-step responses to the hyperpolarizing current step reveals a significant difference for the mutants (red in *B*) compared with controls (black in *B*). (*C*) Quantitation of sag responses and afterdepolarization in control versus mutant animals shows significant increases in *Satb2* mutant neurons compared with controls. (*D–E*) *In situ* hybridization for *HCN1* on coronal E18.5 sections reveals a striking upregulation of *HCN1* expression in the *Satb2*-deficient cortex (*E*) compared with control (*D*). Scale bar: 1 mm in E (*D, E*).

observations suggest that the source of subcortically extending β-galactosidase^{+} axons might actually be Satb2-expressing CPNs that reside in the deep layers.

To directly assess the laminar origins of subcortical axons in the mutants, we first injected fluorescent labeled latex beads into the thalamus of P15 animals for retrograde labeling and analyzed laminar positions of retrogradely labeled neurons 2 days after surgery. Labeled neurons were detected exclusively in Layer 6 of both control mice (Fig. 4*A*) and *Emx1-Cre;Satb2* mutants (Fig. 4*B*). We then injected fluorescent microspheres into the cerebral peduncle at the midbrain/pons junction (to target SCPNs in primary motor cortex M1) and into the anterior pretectal nucleus (to target corticotectal projection neurons) of P15 animals and similarly analyzed the positions of retrogradely labeled cells 2 days later. Strikingly, we did not detect any retrogradely labeled neurons in the superficial layers of *Emx1-Cre;Satb2* mutants; instead we observed labeled cells in Layer 5 of both controls and mutants following injections into the cerebral peduncle (Fig. 4*C,D*) or into the pretectal nucleus (Fig. 4*E,F*). Thus, despite the extensive number of β-galactosidase^{+} axons that extend to subcortical targets in *Satb2* mutants (Supplementary Fig. 2D and F), these retrograde labeling experiments suggest that *Satb2*-expressing neurons in the upper layers do not contribute to these novel projections. Instead, the axons must arise from deep layer *Satb2*-expressing cells, which normally form callosal and corticocortical projections.

Our data suggest that neurons that normally express *Satb2* show a differential ability to form subcerebral projections, depending on their laminar position. Deep layer CPNs can form subcerebral projections in the absence of *Satb2*, but superficial layer CPNs appear unable to do so. To further explore this hypothesis, we utilized a Tamoxifen-inducible *Nestin-Cre*^{ERT2} line (Imayoshi et al. 2006) that targets neural progenitors in a Tamoxifen-dependent manner: early Tamoxifen administration at E11.5 induces recombination in progenitors that will sequentially generate both deep layer neurons and, via later subventricular zone progenitors, neurons of the upper layers (Noctor et al. 2001; Miyata et al. 2001). Late Tamoxifen administration, on the other hand, leads to recombination in the late progenitor pool that gives rise to superficial layer neurons, bypassing already-born deep layer neurons. This enabled us to target Cre-mediated recombination of *Satb2* exclusively to upper layer neurons.

As a control, we first administered 0.3 mg Tamoxifen to pregnant *Nestin-Cre*^{ERT2}*;Ai9*$^{+}$ females at E11.5 and analyzed their offspring at P4. RFP expression was detected in a large fraction of Satb2-expressing neurons of the superficial layers (Supplementary Fig. 5A) and in deep layer pyramidal neurons (Supplementary Fig. 5B), indicating widespread recombination across the cortical wall after a single dose of Tamoxifen. As predicted, a single Tamoxifen administration at E15.5 led to RFP expression predominantly in superficial layers (Supplementary Fig. 5C and E), but, as expected, few if any RFP^{+} neurons were observed in deep layers (Supplementary Fig. 5F).

To compare the effects of ablating *Satb2* in neurons of all layers versus exclusively in upper layer cells, we administered 0.3 mg Tamoxifen to pregnant mice at E11.5 or E15.5 and analyzed *Nestin-Cre*$^{ERT2+}$*;Satb2*$^{lox/lacZ}$ offspring at P4. These brains showed mosaicism for *Satb2*: non-recombined neurons (*Satb2*$^{lox/lacZ}$) have one functional copy of *Satb2* and should extend β-galactosidase^{+} projections across the corpus callosum. *Satb2*$^{\Delta/lacZ}$ recombined neurons (lox allele recombined; Δ), on the other hand, should serve as the origin of β-galactosidase^{+} subcortical projections. In sagittal sections of P4 animals treated with a single Tamoxifen dose at E11.5, which enabled recombination in all layers, β-galactosidase^{+} axons were present in the internal capsule and thalamus (Fig. 4*G*), and in the CST along the brainstem (Fig. 4*I*). However, in animals treated with Tamoxifen at E15.5 to target recombination exclusively to the upper layers, no β-galactosidase^{+} axons were detected in the internal capsule or thalamus (Fig. 4*H*), nor within the brainstem (Fig. 4*J*). These data suggest strongly that *Satb2*-deficient superficial layer neurons lack the capability to form subcortical projections. Collectively our retrograde labeling experiments and timed Tamoxifen *Nestin-Cre*^{ERT2} experiments suggest that the

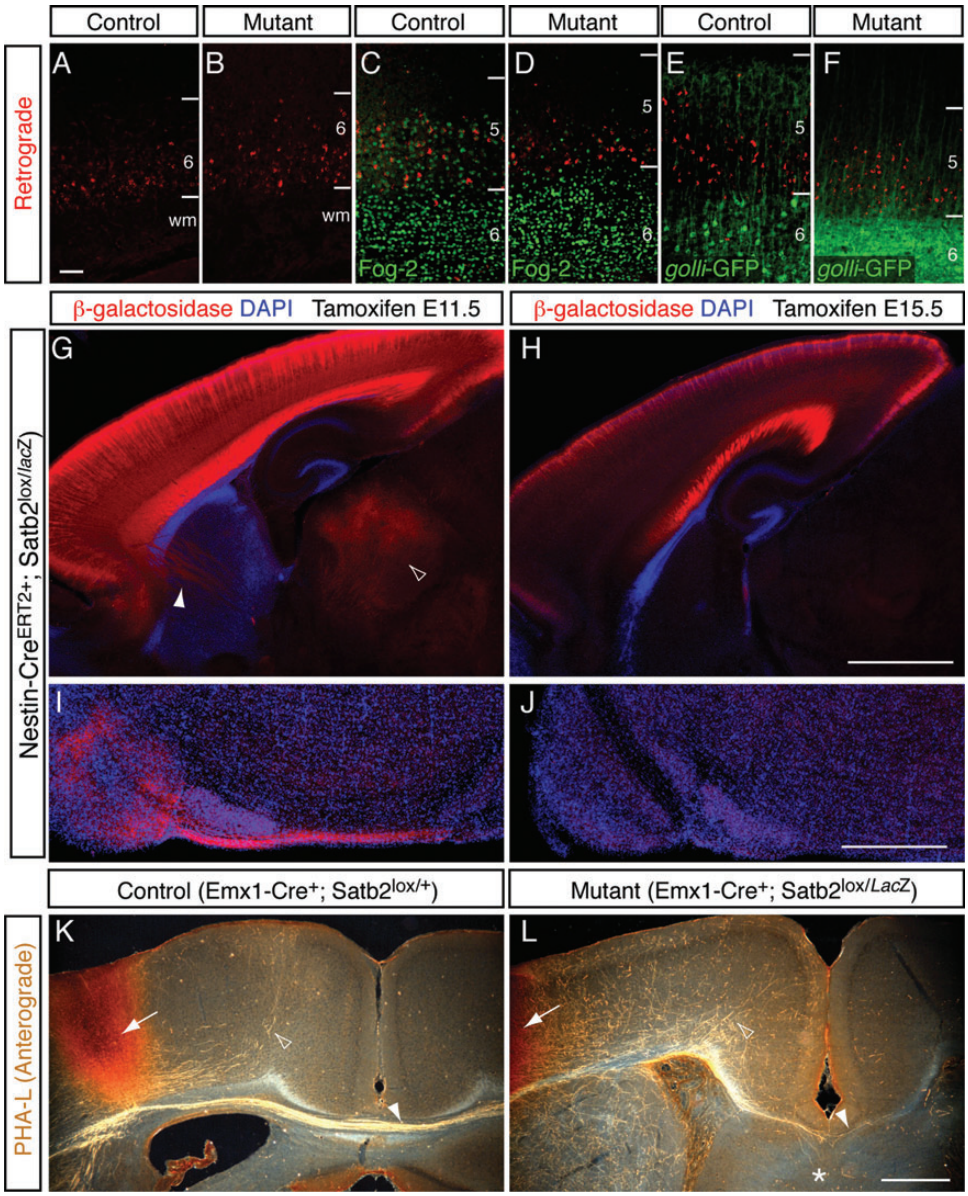

Figure 4. Laminar fate restriction of pyramidal neurons within cortical layers. (*A–F*) Retrograde tracing from subcortical targets reveals laminar restriction of pyramidal neurons in sagittal sections of P17 *Emx1-Cre;Satb2* animals. (*A*, *B*) Retrograde labeling from the thalamus reveals labeled neurons (red in *A*, *B*) in Layer 6 of *Emx1-Cre*$^{+}$*;Satb2*$^{+/lacZ}$ (control; *A*) and *Emx1-Cre*$^{+}$*;Satb2*$^{lox/lacZ}$ (mutant; *B*). (*C*, *D*) Retrograde labeling from the cerebral peduncle at the pons/midbrain junction reveals neurons in Layer 5 (red in *C*, *D*) in control (*C*) and mutant (*D*) *Emx1-Cre;Satb2* animals. Sections were counterstained with Fog-2 (green in *C*, *D*), which shows high expression in Layer 6 and weak expression in some Layer 5 neurons. (*E*, *F*) Backlabeling of neurons in Layer 5 of control (*E*) and mutant (*F*) brains from retrograde injections into the anterior pretectal nucleus. Animals were hemizygous for *golli*-GFP (green in *E*, *F*), which prominently labels neurons of Layer 6 and some Layer 5 neurons. (*G–J*) Tamoxifen-inducible *Nestin-Cre*^{ERT2}*;Satb2* mutants confirm that aberrant subcortical projections in *Satb2* mutants arise from the deep layers, and not from the superficial layers. (*G*, *I*) Sagittal sections of a P4 *Nestin-Cre*^{ERT2}*;Satb2*$^{lox/lacZ}$ mutant treated with a single dose of Tamoxifen at E11.5 reveal β-galactosidase expression (red in *G–J*) across the entire cortical wall (*G*) and β-galactosidase^{+} axons in the internal capsule (arrowhead in *G*), thalamus (open arrowhead in *G*) and along the CST in the brainstem (*I*). (*H*, *J*) Sagittal sections of a P4 *Nestin-Cre*^{ERT2}*;Satb2*$^{lox/lacZ}$ mutant treated with a single dose of Tamoxifen at E15.5 shows β-galactosidase expression confined to superficial layers (*H*) and the absence of β-galactosidase^{+} subcortical axons (*J*), suggesting that *Satb2*-deficient superficial CPNs do not contribute to subcortical projections. (*K*, *L*) Anterograde axonal labeling using *Phaseolus vulgaris* leucoagglutinin (PHA-L) from somatosensory cortex of P15 *Emx1-Cre*$^{+}$*;Satb2*$^{lox/+}$ (control; *K*) and *Emx1-Cre*$^{+}$*;Satb2*$^{lox/lacZ}$ (mutant; *L*) shows labeled axons along the corpus callosum of controls (filled arrowhead in *K*), but a dramatic reduction in mutants (*L*). Instead, mutant axons project ventrally (asterisk in *L*) and an increase in ipsilateral projections (open arrowheads in *K* and *L*) is observed in Emx1-Cre;Satb2 mutants. Arrows in *K* and *L* indicate injection sites. Scale bars: 100 μm in *A* for *A–F*; 1 mm in H (for *G*, *H*); 500 μm in J (for *I*, *J*) and K (for *K*, *L*).

loss of *Satb2* causes deep layer CPNs to project subcortically, but reveal that superficial layer callosal neurons fail to contribute to subcortical β-galactosidase^{+} projections.

To characterize the projection patterns of *Satb2*-deficient CPNs in more detail, we placed injections of an anterograde tracer in the somatosensory cortex of *Emx1-Cre;Satb2* control and mutant animals. *Phaseolus vulgaris* leucoagglutinin (PHA-L) was administered by iontophoretic injection (Gerfen and Sawchenko 1984) at P15, and animals were analyzed 48 h later (Fig. 4*K*,*L*). Although we attempted to selectively label the upper layers, we found that PHA-L also labeled deep layer neurons, perhaps via their dendrites in the superficial layers. PHA-L injections in somatosensory cortex of controls resulted in labeling of both ipsilateral and callosally projecting axons,

as well as axons that extended subcortically (Fig. 4*K*). In *Emx1-Cre;Satb2* mutants, however, very few PHA-L labeled axons were visible in the corpus callosum or contralateral hemisphere; instead we observed a qualitative increase in ipsilateral projections. Many labeled axons in the region of the midline projected ventrally toward the septum, taking a pathway similar to that of β-galactosidase^{+} fibers (Supplementary Fig. 2B), suggesting that some of the *Satb2*-deficient pyramidal neurons aberrantly project into the septum.

A Surprising Role for Satb2 in CST Formation by Layer 5 SCPNs

During our analysis of subcortical connectivity in *Emx1-Cre;Satb2* mutants, we decided to investigate CST formation by taking advantage of the AP marker utilized to generate a null allele of *Fezf2* (*Fezf2^{AP}*), which labels the axonal projections of *Fezf2*$^{+}$ neurons (Chen et al. 2005). We showed previously that *Fezf2* expression is not altered in *Satb2*$^{-/-}$ animals (Alcamo et al. 2008), thus *Fezf2^{AP}* can be used to mark the axons of deep layer SCPNs.

In sagittal sections of P4 brains, *Fezf2^{AP}* labels the CST along the cerebral peduncle, the brainstem, through the pyramidal decussation into the spinal cord (Fig. 5*A*). To our surprise, in *Emx1-Cre;Satb2* mutants carrying the *Fezf2^{AP}* allele, AP activity was not detected caudal of the cerebral peduncle (Fig. 5*B*). Cross sections through the brainstem at 2 separate levels confirmed these findings: in controls, strong AP reactivity was observed at the ventral surface where the pyramids are located (Fig. 5*C*,*C*′), but in *Emx1-Cre;Satb2* mutants, no AP reactivity was found (Fig. 5*D*, *D*′). Ventral views of whole-mount brain preparations further supported the loss of the AP^{+} CST in *Emx1-Cre;Satb2* mutants: controls revealed a robust AP signal in the cerebral peduncle, pyramids and pyramidal decussation (Fig. 5*E*). In *Emx1-Cre;Satb2* mutants, however, AP marked the cerebral peduncle but no signal was detectable in the brainstem (Fig. 5*F*). To determine whether the lack of AP^{+} CST axons in *Emx1-Cre;Satb2* mutants is due to a developmental delay, we analyzed cross sections of the cervical spinal cord at P15. Controls showed strong AP labeling of the CST within the ventral dorsal funiculus (Fig. 5*G*), whereas no signal was detected in *Emx1-Cre;Satb2* mutants (Fig. 5*H*).

To preclude the possibility that *Fezf2^{AP}* might simply be downregulated in the mutants, we labeled the CST at P15 using an antibody against PKCγ, a CST-specific marker (Mori et al. 1990). In control sagittal sections, PKCγ strongly labeled the CST at the cerebral peduncle, through the pyramidal decussation and in the spinal cord (Fig. 5*I*). In *Emx1-Cre;Satb2* mutants, however, strong PKCγ labeling was only found at the cerebral peduncle; weak labeling was found at the level of the pons and very few PKCγ^{+} axons were visible in the brainstem (Fig. 5*J*), suggesting a failure of CST formation at the cerebral peduncle. Immunolabeling of P15 cross sections through the cervical spinal cord revealed robust PKCγ staining in the control CST at the ventral dorsal funiculus, as well as in spinal interneurons (Fig. 5*K*). In *Emx1-Cre;Satb2* mutants, PKCγ expression by interneurons was present but CST labeling was absent (Fig. 5*L*). Taken together, our findings indicate that the *Emx1-Cre*-induced loss of *Satb2* leads to the unexpected failure of *Fezf2*-expressing Layer 5 neurons to extend CST axons past the cerebral peduncle.

Transient Expression of Satb2 in Ctip2^{+} Layer 5 Neurons During Cortical Development

Satb2 function in the developing brain has been associated with the specification of CPNs (Alcamo et al. 2008; Britanova et al. 2008; Baranek et al. 2012), but not with that of SCPNs. The failure of Layer 5 neurons to form a normal CST in *Emx1-Cre;Satb2* mutants suggests either that *Satb2* is playing a non-cell-autonomous role in their development, or that an early, transient, expression of *Satb2* in SCPNs plays a critical role in their differentiation. Our previous studies suggested that as many 40% of Layer 5 neurons coexpress Ctip2 and Satb2 during embryonic development (Alcamo et al. 2008). We reexamined this issue by performing a systematic analysis of Ctip2/Satb2 coexpression between E13.5 and P4. We note that the primary antibodies used here differ from those used previously (Alcamo et al. 2008), which may account for quantitative differences between these 2 studies.

From E13.5, the peak time of Layer 5 neurogenesis, through E15.5, when Satb2 expression is becoming more robust, we find that few Ctip2^{+} cells in the developing cortical plate coexpressed Satb2 (Fig. 6*A*–*F*). Between E16.5 and P4, roughly 20% of Ctip2^{+} neurons also expressed Satb2 (Fig. 6*G*–*J*). After P7, *Satb2* expression in the cortex gradually decreases, and by P15 we were unable to detect either Satb2 protein or β-galactosidase in *Satb2$^{+/lacZ}$* animals (data not shown). These data suggest that Satb2 and Ctip2 are coexpressed in a substantial fraction (20% to 40%, depending on the antibodies employed) of Layer 5 neurons between E16 and P4; these numbers would underestimate the fraction if coexpression is asynchronous within Layer 5. More importantly, these observations raise the possibility that the transient expression of Satb2 in SCPNs might play a role in their normal differentiation.

In support of this hypothesis, we observed alterations in the expression of 2 genes that are normally enriched in SCPNs, the Forkhead box transcription factors *Foxo1* and *Foxp2,* in *Emx1-Cre;Satb2* mutants. *Foxo1*, which is expressed in Layer 5 of control brains (Fig. 7*A*,*A*′) at P1, is lost in *Emx1-Cre;Satb2* mutants (Fig. 7*B*,*B*′). Similarly, *Foxp2*, which is normally expressed in Layers 5 and 6 (Fig. 7*C*,*C*′), is lost in Layer 5 of *Emx1-Cre;Satb2* mutants but its expression is not obviously affected in Layer 6 (Fig. 7*D*,*D*′). The layer 5-specific loss of both transcription factors in *Emx1-Cre;Satb2* mutants indicate that differentiation of Layer 5 SCPNs is incomplete, supporting a role for *Satb2* in the postmitotic differentiation of SCPNs.

Early Transient Expression of Satb2 is Required for SCPN Development

To test its role in SCPN differentiation, we attempted to ablate *Satb2* specifically in Layer 5 neurons at a stage later than that conferred by *Emx1-Cre*, which mediates recombination as early as E10.5 (Gorski et al. 2002). The BAC transgenic line *Rbp4-Cre* (Gong et al. 2007) targets Layer 5 neurons (Kozorovitskiy et al. 2012; Glickfeld et al. 2013); however, a detailed characterization of the line and the onset of Cre activity have not yet been described. We first investigated the specificity and timing of *Rbp4-Cre*-mediated recombination using the *Ai9* reporter. In *Rbp4-Cre^{+};Ai9^{+}* animals, RFP^{+} neurons were detected as early as E16.5 (Fig. 8*A*,*B*); however, at E16.5 and E17.5, only a small fraction of Ctip2^{+} neurons expressed RFP (Fig. 8*C*). By P4, RFP expression in Layer 5 was robust and widespread, and the majority of Ctip2^{+} neurons were marked

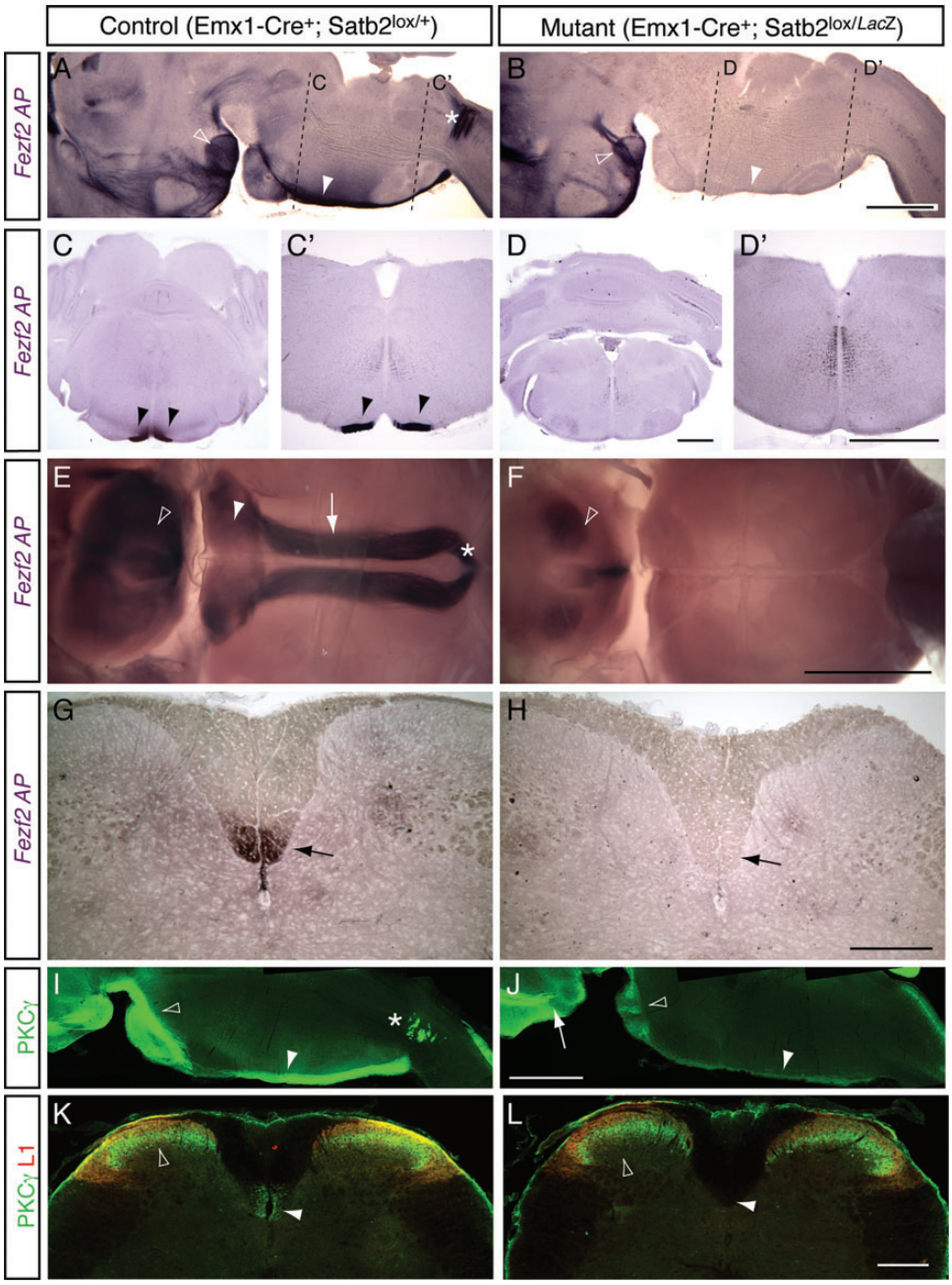

Figure 5. Loss of *Satb2* leads to a failure of the CST. (*A–H*) *Emx1-Cre;Satb2* animals heterozygous for *Fezf2*^{AP} allow visualization of the CST using AP. (*A*, *B*) Sagittal sections of P4 brains reveal AP^{+} CST axons within the cerebral peduncle (open arrowheads in *A*, *B*). (*A*) In *Emx1-Cre*$^{+}$*;Satb2*$^{lox/+}$*;Fezf2*^{AP} controls, the CST can be observed in the ventral brainstem (arrowhead in *A*) and crossing into the spinal cord at the pyramidal decussation (asterisk in *A*). In *Emx1-Cre*$^{+}$*;Satb2*$^{lox/LacZ}$*;Fezf2*^{AP} mutants, labeling is present in the cerebral peduncle (open arrowhead in *B*), but no AP is detected in the brainstem (arrowhead in *B*) or pyramidal decussation. (*C*, *D*) Cross sections through the brainstem at the levels indicated by the dashed lines in *A* and *B* reveal the AP^{+} CST at the ventral surface of controls (arrowheads in *C* and *C'*), but a loss of the CST in *Emx1-Cre;Satb2* mutants (*D*, *D'*). (*E*, *F*) Whole-mount ventral views of AP histochemistry on P4 brains confirm the failure of CST formation in *Emx1-Cre;Satb2* mutants. In controls, AP staining marks CST axons in the cerebral peduncle (open arrowhead in *E*), along the pons (arrowhead in *E*), the pyramids (arrow in *E*), and pyramidal decussation (asterisk in *E*). In *Satb2*-deficient animals, some AP reactivity is found at the cerebral peduncle (open arrowhead in *F*), but the tract fails to extend into the brainstem (*F*). (*G*, *H*) Cross sections through cervical spinal cord of P15 animals reveal a loss of CST axons in *Emx1-Cre;Satb2* mutants. In controls, AP labels CST axons in the ventral dorsal funiculus (arrow in *G*), but no AP signal is detected in the mutant spinal cord (arrow in *H*). (*I–L*) Protein kinase C γ (PKCγ) immunohistochemistry confirms the loss of CST in *Satb2* mutants. Immunohistological analysis of P15 sagittal brain sections reveals the PKCγ^{+} CST in controls at the level of the cerebral peduncle, pons (open arrowhead in I), pyramids (arrowhead in *I*), and pyramidal decussation (asterisk in *I*). In *Emx1-Cre;Satb2* mutants, strong PKCγ labeling is found in the cerebral peduncle (arrow in *J*), but only weak label at the pons (open arrowhead in *J*) and very weak signal along the pyramids (arrowhead in *J*). (*K*, *L*) Cross sections through cervical spinal cord of P15 animals reveals PKCγ labeling of the CST in the ventral dorsal funiculus of controls (arrowhead in *K*), but the absence of the tract in mutants (arrowhead in *L*). PKCγ is also expressed by interneurons of the spinal cord (open arrowheads in *K*, *L*). Sections were colabeled with L1. Scale bars: 1 mm in *B* (*A*, *B*), *D* (*C*, *D*), *D'* (*C'*, *D'*), *F* (*E*, *F*), 250 μm in *H* (*G*, *H*), 1 mm in *J* (*I*, *J*), 250 μm in *L* (*K*, *L*).

with RFP (Fig. 8*D–F*). The axonal transport of RFP labeled the internal capsule (Fig. 8*D*), cerebral peduncle (Fig. 8*H*), pyramidal decussation, and CST (Fig. 8*I*); RFP was also present in the anterior commissure (Fig. 8*G*), indicating that *Rbp4-Cre* recombines both SCPNs and commissural neurons of Layer 5. These results demonstrate that *Rbp4-Cre* shows a high specificity for

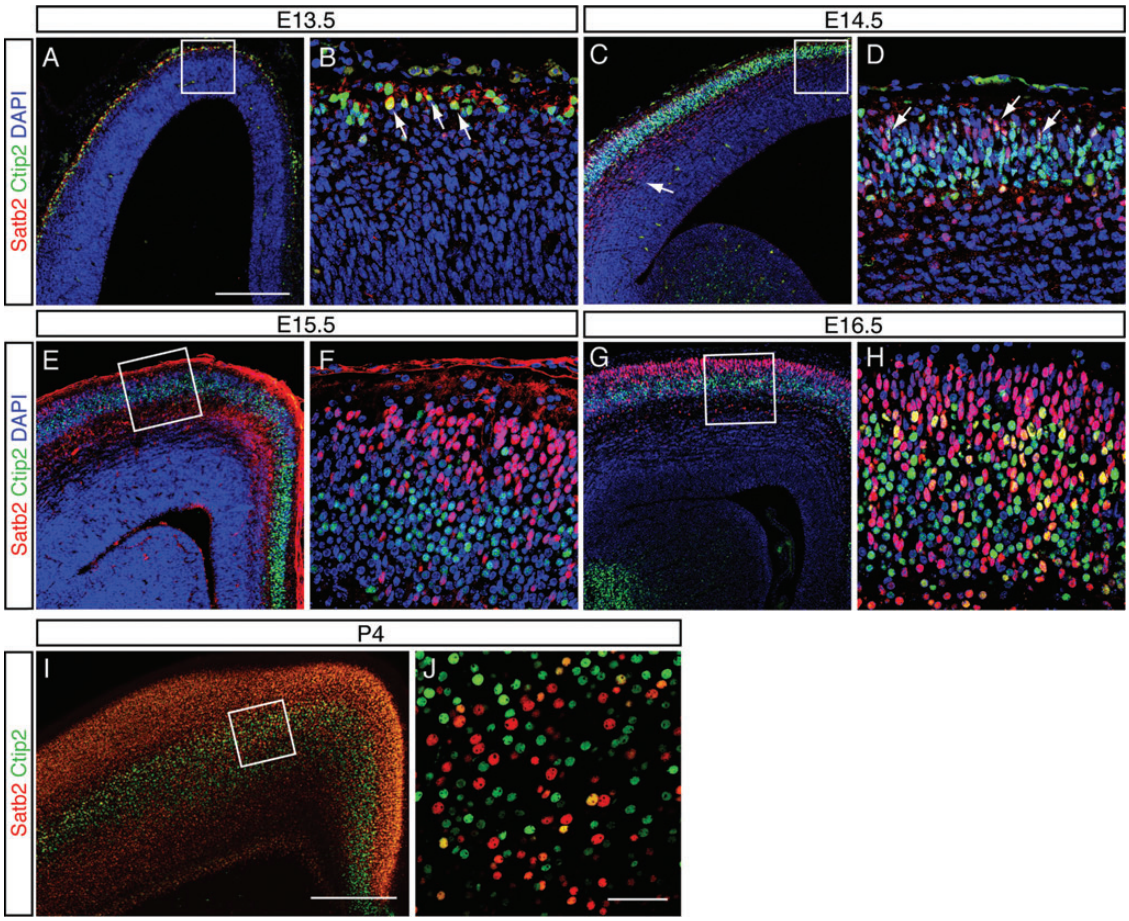

Figure 6. Colocalization of Satb2 and Ctip2 during embryonic development suggests early role of Satb2 in corticospinal motor neuron differentiation. (*A–L*) Immunohistological analysis of Satb2 (red in *A–J*) and Ctip2 (green in *A–J*) reveals overlap during embryonic development of the cerebral cortex. (*A*, *B*) At E13.5, the time when Layer 5 neurons are being born, very little Satb2 immunoreactivity is observed in the cerebral cortex (*A*). At high power magnification (*B*; boxed area in *A*), few Ctip2$^+$ cells coexpress Satb2 (arrows in *B*). (*C*, *D*) At E14.5, Satb2 expression emerges more robustly, with highest expression levels found in the lateral areas of developing cortex (arrow in *C*). (*D*) In motor cortex (boxed area in *C*), some Ctip2$^+$ cells coexpress Satb2 (arrows in *D*). (*E*, *F*) At E15.5, Satb2 expression has expanded from lateral neocortex into motor cortex, and Satb2 marks the majority of neurons in developing Layer 4. (*G*, *H*) At E16.5, robust Satb2 expression is apparent in the developing upper layers of the cerebral cortex. High power magnification (*H*; boxed area in *G*) reveals considerable overlap between Satb2 and Ctip2 in maturing Layer 5 neurons. (*I*, *J*) at P4, robust Satb2 expression is observed across the entire cortical wall (*I*) and magnification of Layer 5 (*J*; boxed area in *I*) shows a fraction of Ctip2$^+$ neurons coexpressing Satb2. Scale bars: 250 μm in *A* (*A*, *C*, *E*, *G*), 500 μm in I, 50 μm in *J* (*B*, *D*, *F*, *H*, *J*).

Layer 5 neurons. The earliest activity on the reporter allele was detected at E16.5, several days after the birth of Layer 5 neurons at around E13.5, suggesting that *Rbp4-Cre* ablates target genes during Layer 5 neuron differentiation and maturation.

To assess whether *Rbp4-Cre* effectively ablates *Satb2* in Layer 5, we analyzed *Rbp4-Cre;Satb2;Ai9* animals for Satb2 and RFP at P4. In controls, RFP was readily observed in Layer 5 (Fig. 9*A*), where some cells colocalized RFP and Satb2 (Fig. 9*A′*, similar to the coexpression of Ctip2 and Satb2 in wildtype mice in Fig. 6*J*). In *Rbp4-Cre;Satb2* mutants, however, the fraction of RFP$^+$ neurons that expressed Satb2 was dramatically reduced (Fig. 9*B′*), indicating that *Rbp4-Cre* efficiently ablates *Satb2* in the RFP$^+$ population.

To investigate whether late *Rbp4-Cre*-mediated recombination phenocopies the failure of CST development observed in *Emx1-Cre;Satb2* mutants, we analyzed both lines at P4 using the Ai9 reporter to specifically label the axons of recombined neurons. In control *Emx1-Cre* mice that were heterozygous for *Satb2*, RFP marked subcortical axons of the CST in the brainstem and pyramidal decussation (Fig. 9*C*). In *Emx1-Cre;Satb2* mutant littermates, however, robust RFP expression terminated at the cerebral peduncle; only very weak signal was visible in the brainstem (Fig. 9*D*; compare with Fig. 5*B*,*F*,*J*). In the *Rbp4-Cre;Satb2* strain, on the other hand, RFP robustly marked CST axons extending through the brainstem, pyramidal decussation and into the spinal cord of both controls and mutants (Fig. 9*E*,*F*).

To investigate CST development more caudally in both strains, we immunolabeled sections through the spinal cord of P15 animals for RFP and PKCγ. In *Emx1-Cre;Satb2* heterozygous controls, the ventral dorsal funiculus showed strong labeling with both markers (Fig. 9*G*). In *Emx1-Cre;Satb2* mutants, however, neither RFP nor PKCγ was detectable (Fig. 9*H*), confirming the failure of the CST rostrally. In *Rbp4-Cre;Satb2* mice, RFP and PKCγ labeled the CST in both controls and mutants (Fig. 9I,*J*), suggesting that *Satb2* is dispensable during the late maturation (from ~E17.5 to P4) of Layer 5 SCPNs. Since results from *Emx1-Cre;Satb2* mutants demonstrate that *Satb2* is required for normal CST formation, our data are consistent with the possibility that the transient expression of Satb2 in layer 5 SCPNs plays an unexpected, cell-autonomous role early in their differentiation, before E17.5. Additional studies will be required to rule out non-cell-autonomous functions.

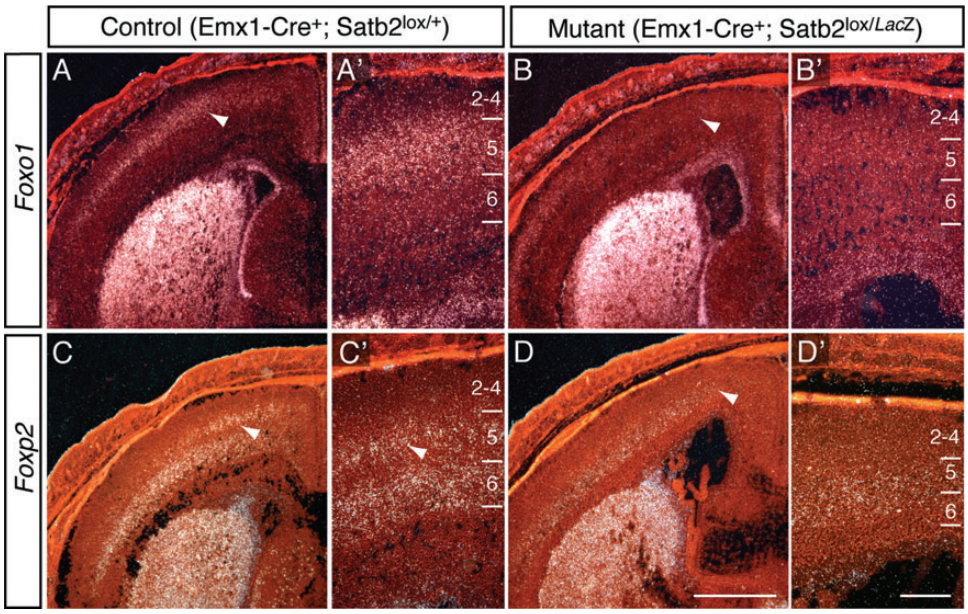

Figure 7. Molecular changes in Layer 5 of *Emx1-Cre;Satb2* mutants suggest incomplete differentiation of SCPNs. *In situ* hybridization on coronal P1 sections shows a loss of the SCPN differentiation markers *Foxo1* (*A–B*) and *Foxp2* (*C–D*) in Layer 5 motor cortex (arrowheads in *A–D*) of *Emx1-Cre*$^{+}$*;Satb2*$^{lox/LacZ}$ mutants (*B*, *D*) compared with Emx1-Cre^{+}; Satb2$^{lox/+}$ controls (*A*, *C*). High power magnification reveals expression of *Foxo1* in Layer 5 of controls (*A′*) and loss of *Foxo1* in Layer 5 motor cortex of *Emx1-Cre;Satb2* mutants (*B′*). *Foxp2* expression is detected in both Layer 5 (arrowhead in *C′*) and Layer 6 of control animals, but is lost specifically in Layer 5 of *Emx1-Cre;Satb2* mutants (*D′*). Scale bars: 1 mm in D for *A–D*, 100 μm in *D′* for *A′–D′*.

Discussion

Previous studies of the chromatin-remodeling protein Satb2 have focused on its role in regulating the specification and differentiation of callosal projection neurons in the developing neocortex (Alcamo et al. 2008; Britanova et al. 2008; Gyorgy et al. 2008; Srinivasan et al. 2012). We have broadened these studies and extended them into novel realms. Using a conditional allele of *Satb2* in combination with the cortex-specific *Emx1-Cre* driver, we first found that the β-galactosidase^{+} axons of *Satb2*-expressing neurons are capable of extending into the CST during postnatal life, further demonstrating that CPNs can adopt an SCPN fate in the absence of *Satb2*. Surprisingly, though, retrograde labeling studies and the use of different Cre driver lines revealed that these novel projections arise exclusively from the deep layers of cortex, and not from the upper layers. Thus, although the loss of *Satb2* leads to electrophysiological changes in superficial layer neurons and upregulation of several genes normally expressed in Layer 5, our studies reveal that upper layer neurons are unable to convert entirely to an SCPN fate—their axons do not extend subcortically.

Distinct Developmental Potentials of Upper and Deep Layer Cortical Neurons

Our results suggest that the populations of *Satb2*-expressing neurons in the upper and deep layers are fundamentally different, despite their molecular similarities. Perhaps this ought not to have been surprising since superficial layer CPNs are a recent acquisition during evolution, first observed in placental mammals (reviewed in Aboitiz and Montiel 2003 and Fame et al. 2011). In addition, it has long been appreciated that deep layer CPNs are generated side by side with SCPNs from *Fezf2*-expressing progenitor cells; it seems reasonable that deep layer CPNs retain enough of their genetic heritage to project subcortically in the absence of *Satb2*. Superficial layer neurons, on the other hand, are derived from the evolutionary recent cortical expansion involving the emergence of the subventricular zone (SVZ). A number of genes and molecular markers are uniquely associated with SVZ progenitors and their superficial layer progeny, including Tbr2 (Baala et al. 2007; Arnold et al. 2008; Sessa et al. 2008), *Svet1* (Tarabykin et al. 2001), and Cux1 and Cux2 (Zimmer et al. 2004; Cubelos et al. 2010). While SVZ and upper layer cells might retain or reuse genes like *Satb2* that are part of an evolutionarily more ancient genetic program, the interpretation of this program may differ profoundly in the context of a distinct transcriptional and layer-specific environment.

The concept that *Satb2* has been "redeployed" by neurons in the evolutionary recent superficial layers helps to reconcile previous models of inhibitory interactions between *Fezf2, Satb2*, and *Ctip2* (Alcamo et al. 2008; Britanova et al. 2008; Gyorgy et al. 2008; Chen et al. 2008; Srinivasan et al. 2012) with the current data. Our findings suggest that these genetic interactions are cell-type and context dependent—indeed, one key difference between deep and upper layer neurons is that the protooncogene *Ski* is coexpressed with *Satb2* in superficial layers, and Ski plays a critical role in enabling Satb2 to form a repressor complex in situ (Baranek et al. 2012). Satb2 binds to MAR in regulatory sequences of *Ctip2* and represses *Ctip2* by assembling 2 members of the nucleosome remodeling and deacetylase (NuRD) complex, the histone deacetylases HDAC1 and MTA2 (Alcamo et al. 2008; Britanova et al. 2008). Ski is not required for the interaction between Satb2 and the MAR sequences, however, it is required for the recruitment of HDAC1, thereby allowing the NuRD complex to assemble, which then leads to the repression of *Ctip2*.

These studies suggest that the presence of Ski in superficial layer neurons enables the formation of a Satb2/Ski/NuRD complex and the efficient repression of *Ctip2*. In addition, upper layer neurons fail to express critical deep layer determinants such as *Fezf2*, even in the absence of *Satb2* function.

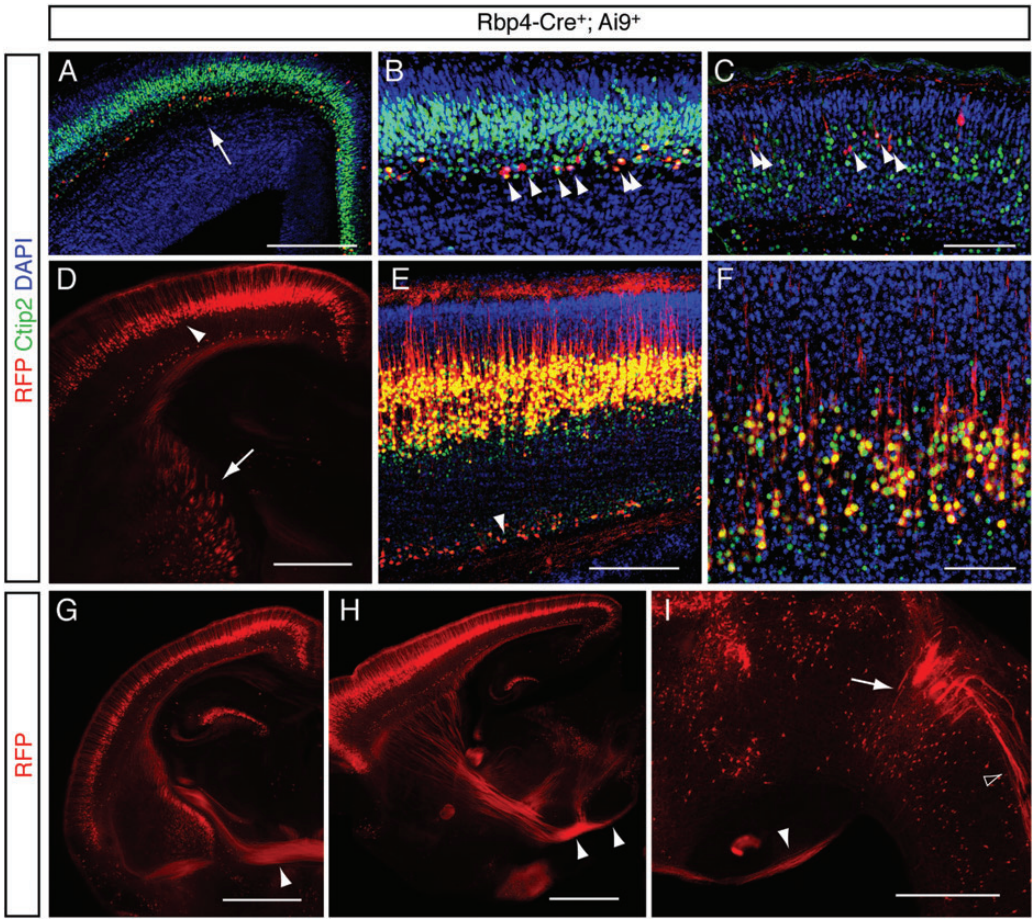

Figure 8. *Rbp4-Cre* targets recombination to Layer 5 pyramidal neurons. *Rbp4-Cre* activity was assessed by *Ai9-RFP* expression in *Rbp4-Cre*$^{+}$;*Ai9*$^{+}$ animals. (*A–F*) Immunohistological analysis of RFP (in red in *A–I*) and Ctip2 (green in *A–F*) shows the onset of RFP expression in coronal sections of E16.5 brains (*A*, *B*). (*A*) Very few RFP^{+} cells are seen in the developing cortex at E16.5. (*B*) High power magnification of motor cortex shows that the majority of RFP^{+} neurons coexpress Ctip2 (arrowheads in *B*). (*C*) At E17.5, only a fraction of Ctip2^{+} neurons coexpress RFP. (*D–F*) Coronal sections of P4 animals show robust RFP expression in Layer 5 neurons (arrowhead in *D*) and RFP^{+} axons in the internal capsule (arrow in *D*). (*E*) The majority of Ctip2^{+} neurons coexpress RFP; some RFP^{+} cells are also found above the white matter (arrowhead in *E*). (*F*) High power magnification of Layer 5 reveals that the majority of the large Ctip2^{+} Layer 5 neurons coexpress RFP, and the majority of the RFP^{-};Ctip2^{+} neurons are neurons with smaller nuclei. (*G*) A coronal section of a P4 brain shows RFP in the anterior commissure (arrowhead in *G*). (*H*, *I*) Sagittal sections of P4 brains reveal RFP^{+} axons in the cerebral peduncle (arrowheads in *H*), in the CST in the brainstem (arrowhead in *I*), in the pyramidal decussation (arrow in *I*) and in descending fibers in the spinal cord (open arrowhead in *I*). Scale bars: 250 μm in *A* and *E*; 100 μm in *C* for *B*, *C*; 50 μm in *F*; 1 mm in *D*, *G* and *H*; 500 μm in *I*.

The presence of *Ski* and absence of *Fezf2* expression may account for the inability of upper layer neurons to completely adopt an SCPN fate in the absence of *Satb2*.

In the deep layers, on the other hand, the percentage of Ski^{+};Satb2^{+} neurons is much lower than in the superficial layers, suggesting that *Satb2* may function independently of *Ski* (Baranek et al. 2012). Indeed, the substantial coexpression of Satb2 and Ctip2 in Layer 5 neurons during development suggests that Satb2 is less effective in inhibiting *Ctip2* expression compared with cells in the upper layers. Satb proteins can regulate gene expression by activating or repressing transcription and by altering chromatin structure (Cai et al. 2003, 2006; Dobreva et al. 2006), and we speculate that Satb2 may function in deep layer neurons by recruiting as yet unidentified partners in the regulation of target gene expression.

An Unexpected Role for Satb2 in the Development of Layer 5 SCPNs

Our experiments unveiled an unexpected role for *Satb2* in the differentiation of Layer 5 SCPNs. In *Satb2* mutant animals, the expression of several Layer 5 differentiation markers was reduced compared with wildtype controls, indicating an incomplete differentiation of *Satb2*-deficient SCPNs. These molecular changes were accompanied by a failure of the CST to extend past the cerebral peduncle and into the spinal cord. The use of a Layer 5-specific Cre driver showed that the ablation of *Satb2* at relatively late stages of Layer 5 differentiation failed to disrupt CST formation, whereas recombination at early times resulted in a CST phenotype. These data are consistent with the possibility that the transient expression of Satb2 in differentiating SCPNs may actually be required for their normal development. However, further experiments will be needed to rule out a non-cell-autonomous role.

We previously demonstrated that several axon guidance ligands and receptors show altered expression in *Satb2*-deficient brains, and in particular we observed a dramatic reduction in the expression of *Unc5b3* and *EphA4* (Alcamo et al. 2008). Both receptors have been implicated in CST development and pathfinding (reviewed in Harel and Strittmatter 2006): in both *Unc5b3* and *EphA4* mutants, most CST axons terminate along the medulla, rostral to the pyramidal

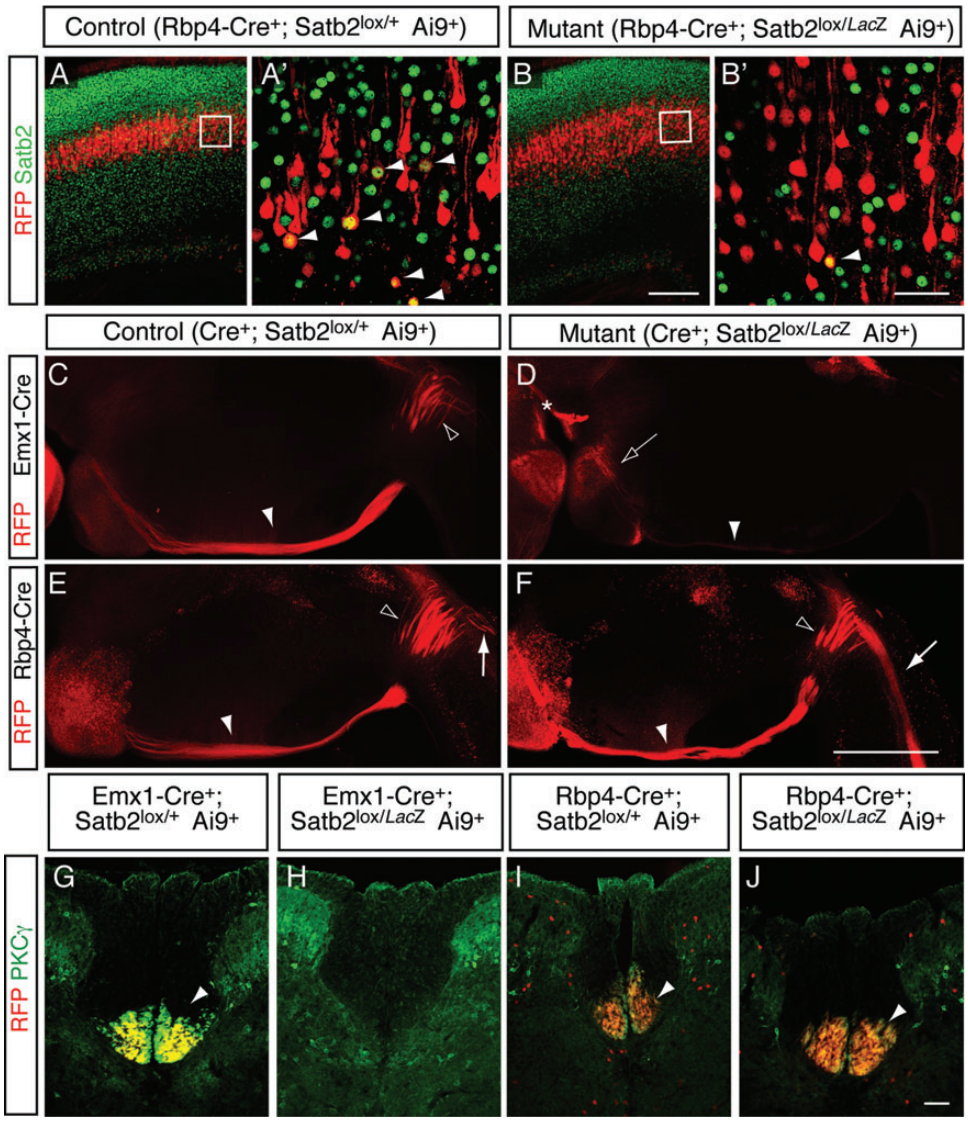

Figure 9. Early *Satb2* expression is required for proper CST development. The *Ai9-RFP* reporter allele was used to visualize Cre-recombined neurons and corticospinal tracts in different mutant *Satb2* strains. (*A*–*B*′) Coronal sections of P4 brains were analyzed for recombination efficiency in *Rbp4-Cre*$^{+}$;*Satb2*$^{lox/+}$;*Ai9*$^{+}$ controls (*A*, *A*′) and *Rbp4-Cre*$^{+}$;*Satb2*$^{lox/LacZ}$;*Ai9*$^{+}$ mutants (*B*, *B*′), respectively. (*A*, *B*) Low power magnification views show Satb2 expression (green in *A*–*B*′) in all cortical layers of both control and mutant, and *Rbp4-Cre*-induced RFP expression (from the *Ai9* reporter) in Layer 5 neurons of both genotypes. (*A*′, *B*′) High power magnification of boxed areas in *A* and *B*. In controls, a subset of RFP^{+} Layer 5 neurons coexpressed Satb2 (arrowheads in *A*′), similar to the coexpression of Satb2 and Ctip2 in Figure 6. (*B*′) In *Rbp4-Cre;Satb2* mutants, the fraction of Satb2^{+};RFP^{+} neurons is dramatically reduced. The small number of Satb2^{+};RFP^{+} neurons (arrowhead in *B*′) may reflect a slow Satb2 protein turnover in Cre-recombined postmitotic neurons. Satb2^{+};RFP^{-} neurons (green in *B*′) are CPNs that are not targeted by *Rbp4-Cre*. (*C*, *D*) Early recombination using *Emx1-Cre* reveals RFP^{+} CST axons in sagittal sections along the brainstem (arrowhead in *C*) and in the pyramidal decussation (open arrowhead in *C*) of P4 *Emx1-Cre*$^{+}$;*Satb2*$^{lox/+}$;*Ai9*$^{+}$ controls (*C*). In *Emx1-Cre*$^{+}$;*Satb2*$^{lox/LacZ}$;*Ai9*$^{+}$ mutants, labeled axons occupy the cerebral peduncle (asterisk in *D*), but few labeled axons are visible at the pons (open arrow in *D*) or brainstem (arrowhead in *D*). (*E*, *F*) Late, Layer 5 specific recombination using *Rbp4-Cre* robustly labels the CST along the brainstem (arrowheads in *E*, *F*), pyramidal decussation (open arrowheads in *E*, *F*) and in descending fibers of the spinal cord (arrows in *E*, *F*) of both control (*E*) and mutant (*F*) animals at P4. (*G*–*J*) RFP and PKCγ immunohistochemistry on cross sections through the cervical spinal cord of P15 animals: (*G*, *H*) Early recombination with *Emx1-Cre* leads to robust RFP expression in the control CST within the ventral dorsal funiculus, which colabels with PKCγ (*G*). In mutants both PKCγ and RFP are missing, suggesting the CST fails to reach the spinal cord (*H*). (*I*, *J*) In contrast, late recombination induced by *Rbp4-Cre* does not disrupt CST development; RFP and PKCγ are detected in the ventral dorsal funiculus in both controls (*I*) and mutants (*J*). Scale bars: 250 μm in *B* for *A*, *B*; 50 μm in *B*′ for *A*′, *B*′; 1 mm in *F* for *C*–*F*; 100 μm in *J* for *G*–*J*.

decussation (Finger et al. 2002; Dottori et al. 1998), a phenotype quite similar to that observed here. It is therefore tempting to speculate that the loss of *Unc5h3* and *EphA4* expression in *Satb2* mutants (Alcamo et al. 2008) leads to defects in axon guidance by SCPNs and a failure of normal CST formation. Whether Satb2 directly regulates the expression of *Unc5h3* and *EphA4* in Layer 5 neurons remains to be determined.

Supplementary Material

Supplementary material can be found at: http://www.cercor.oxfordjournals.org/.

Funding

This work was supported by grants from the National Institutes of Health (EY08411 and MH051864)

Notes

We are grateful to Dr James Weimann for technical help with retrograde tracing and Dr Chris Kaznowski for technical help. We would also like to thank Dr Elizabeth Alcamo for previous experiments. *Conflict of Interest*: None declared.

References

Aboitiz F, Montiel J. 2003. One hundred million years of interhemispheric communication: the history of the corpus callosum. Braz J Med Biol Res. 36:409–420.

Alcamo EA, Chirivella L, Dautzenberg M, Dobreva G, Fariñas I, Grosschedl R, McConnell SK. 2008. Satb2 regulates callosal projection neuron identity in the developing cerebral cortex. Neuron. 57:364–377.

Arlotta P, Molyneaux BJ, Chen J, Inoue J, Kominami R, Macklis JD. 2005. Neuronal subtype-specific genes that control corticospinal motor neuron development in vivo. Neuron. 45:207–221.

Arnold SJ, Huang GJ, Cheung AF, Era T, Nishikawa S, Bikoff EK, Molnár Z, Robertson EJ, Groszer M. 2008. The T-box transcription factor Eomes/Tbr2 regulates neurogenesis in the cortical subventricular zone. Genes Dev. 22:2479–2484.

Baala L, Briault S, Etchevers HC, Laumonnier F, Natiq A, Amiel J, Boddaert N, Picard C, Sbiti A, Asermouh A et al. 2007. Homozygous silencing of T-box transcription factor EOMES leads to microcephaly with polymicrogyria and corpus callosum agenesis. Nat Genet. 39:454–456.

Baranek C, Dittrich M, Parthasarathy S, Bonnon CG, Britanova O, Lanshakov D, Boukhtouche F, Sommer JE, Colmenares C, Tarabykin V et al. 2012. Protooncogene Ski cooperates with the chromatin-remodeling factor Satb2 in specifying callosal neurons. Proc Natl Acad Sci U S A. 109:3546–3551.

Britanova O, de Juan Romero C, Cheung A, Kwan KY, Schwark M, Gyorgy A, Vogel T, Akopov S, Mitkovski M, Agoston D et al. 2008. Satb2 is a postmitotic determinant for upper-layer neuron specification in the neocortex. Neuron. 57:378–392.

Cai S, Han HJ, Kohwi-Shigematsu T. 2003. Tissue-specific nuclear architecture and gene expression regulated by SATB1. Nat Genet. 34:42–51.

Cai S, Lee CC, Kohwi-Shigematsu T. 2006. SATB1 packages densely looped, transcriptionally active chromatin for coordinated expression of cytokine genes. Nat Genet. 38:1278–1288.

Chen B, Schaevitz LR, McConnell SK. 2005. Fezl regulates the differentiation and axon targeting of layer 5 subcortical projection neurons in cerebral cortex. Proc Natl Acad Sci U S A. 102:17184–17189.

Chen B, Wang SS, Hattox AM, Rayburn H, Nelson SB, McConnell SK. 2008. The Fezf2-Ctip2 genetic pathway regulates the fate choice of subcortical projection neurons in the developing cerebral cortex. Proc Natl Acad Sci U S A. 105:11382–11387.

Chen JG, Rasin MR, Kwan KY, Sestan N. 2005. Zfp312 is required for subcortical axonal projections and dendritic morphology of deep-layer pyramidal neurons of the cerebral cortex. Proc Natl Acad Sci U S A. 102:17792–17797.

Cubelos B, Sebastián-Serrano A, Beccari L, Calcagnotto ME, Cisneros E, Kim S, Dopazo A, Alvarez-Dolado M, Redondo JM, Bovolenta P et al. 2010. Cux1 and Cux2 regulate dendritic branching, spine morphology, and synapses of the upper layer neurons of the cortex. Neuron. 66:523–535.

Dembrow NC, Chitwood RA, Johnston D. 2010. Projection-specific neuromodulation of medial prefrontal cortex neurons. J Neurosci. 30:16922–16937.

Dobreva G, Chahrour M, Dautzenberg M, Chirivella L, Kanzler B, Fariñas I, Karsenty G, Grosschedl R. 2006. SATB2 is a multifunctional determinant of craniofacial patterning and osteoblast differentiation. Cell. 125:971–986.

Dobreva G, Dambacher J, Grosschedl R. 2003. SUMO modification of a novel MAR-binding protein, SATB2, modulates immunoglobulin mu gene expression. Genes Dev. 17:3048–3061.

Dottori M, Hartley L, Galea M, Paxinos G, Polizzotto M, Kilpatrick T, Bartlett PF, Murphy M, Köntgen F, Boyd AW. 1998. EphA4 (Sek1) receptor tyrosine kinase is required for the development of the corticospinal tract. Proc Natl Acad Sci U S A. 95:13248–13253.

Fame RM, MacDonald JL, Macklis JD. 2011. Development, specification, and diversity of callosal projection neurons. Trends Neurosci. 34:41–50.

Finger JH, Bronson RT, Harris B, Johnson K, Przyborski SA, Ackerman SL. 2002. The netrin 1 receptors Unc5h3 and Dcc are necessary at multiple choice points for the guidance of corticospinal tract axons. J Neurosci. 22:10346–10356.

Fothergill T, Donahoo AL, Douglass A, Zalucki O, Yuan J, Shu T, Goodhill GJ, Richards LJ. 2013. Netrin-DCC signaling regulates corpus callosum formation through attraction of pioneering axons and by modulating Slit2-mediated repulsion. Cereb Cortex. 24:1138–1151.

Frantz GD, Weimann JM, Levin ME, McConnell SK. 1994. Otx1 and Otx2 define layers and regions in developing cerebral cortex and cerebellum. J Neurosci. 14:5725–5740.

Gerfen CR, Sawchenko PE. 1984. An anterograde neuroanatomical tracing method that shows the detailed morphology of neurons, their axons and terminals: immunohistochemical localization of an axonally transported plant lectin, *Phaseolus vulgaris* leucoagglutinin (PHA-L). Brain Res. 290:219–238.

Glickfeld LL, Andermann ML, Bonin V, Reid RC. 2013. Cortico-cortical projections in mouse visual cortex are functionally target specific. Nat Neurosci. 16:219–226.

Gong S, Doughty M, Harbaugh CR, Cummins A, Hatten ME, Heintz N, Gerfen CR. 2007. Targeting Cre recombinase to specific neuron populations with bacterial artificial chromosome constructs. J Neurosci. 27:9817–9823.

Gorski JA, Talley T, Qiu M, Puelles L, Rubenstein JL, Jones KR. 2002. Cortical excitatory neurons and glia, but not GABAergic neurons, are produced in the Emx1-expressing lineage. J Neurosci. 22:6309–6314.

Greig LC, Woodworth MB, Galazo MJ, Padmanabhan H, Macklis JD. 2013. Molecular logic of neocortical projection neuron specification, development and diversity. Nat Rev Neurosci. 14:755–769.

Gyorgy AB, Szemes M, de Juan Romero C, Tarabykin V, Agoston DV. 2008. SATB2 interacts with chromatin-remodeling molecules in differentiating cortical neurons. Eur J Neurosci. 27:865–873.

Han W, Kwan KY, Shim S, Lam MM, Shin Y, Xu X, Zhu Y, Li M, Sestan N. 2011. TBR1 directly represses Fezf2 to control the laminar origin and development of the corticospinal tract. Proc Natl Acad Sci U S A. 108:3041–3046.

Harel NY, Strittmatter SM. 2006. Can regenerating axons recapitulate developmental guidance during recovery from spinal cord injury?. Nat Rev Neurosci. 7:603–616.

Hevner RF, Shi L, Justice N, Hsueh Y, Sheng M, Smiga S, Bulfone A, Goffinet AM, Campagnoni AT, Rubenstein JL. 2001. Tbr1 regulates differentiation of the preplate and layer 6. Neuron. 29:353–366.

Imayoshi I, Ohtsuka T, Metzger D, Chambon P, Kageyama R. 2006. Temporal regulation of Cre recombinase activity in neural stem cells. Genesis. 44:233–238.

Jacobs EC, Campagnoni C, Kampf K, Reyes SD, Kalra V, Handley V, Xie YY, Hong-Hu Y, Spreur V, Fisher RS et al. 2007. Visualization of corticofugal projections during early cortical development in a tau-GFP-transgenic mouse. Eur J Neurosci. 25:17–30.

Joshi PS, Molyneaux BJ, Feng L, Xie X, Macklis JD, Gan L. 2008. Bhlhb5 regulates the postmitotic acquisition of area identities in layers II-V of the developing neocortex. Neuron. 60:258–272.

Kasper EM, Lübke J, Larkman AU, Blakemore C. 1994. Pyramidal neurons in layer 5 of the rat visual cortex. III. Differential maturation of axon targeting, dendritic morphology, and electrophysiological properties. J Comp Neurol. 339:495–518.

Koester SE, O'Leary DD. 1994. Axons of early generated neurons in cingulate cortex pioneer the corpus callosum. J Neurosci. 14:6608–6620.

Kozorovitskiy Y, Saunders A, Johnson CA, Lowell BB, Sabatini BL. 2012. Recurrent network activity drives striatal synaptogenesis. Nature. 485:646–650.

Kwan KY, Lam MM, Krsnik Z, Kawasawa YI, Lefebvre V, Sestan N. 2008. SOX5 postmitotically regulates migration, postmigratory differentiation, and projections of subplate and deep-layer neocortical neurons. Proc Natl Acad Sci U S A. 105:16021–16026.

Lai T, Jabaudon D, Molyneaux BJ, Azim E, Arlotta P, Menezes JR, Macklis JD. 2008. SOX5 controls the sequential generation of distinct corticofugal neuron subtypes. Neuron. 57:232–247.
Larkman A, Mason A. 1990. Correlations between morphology and electrophysiology of pyramidal neurons in slices of rat visual cortex. I. Establishment of cell classes. J Neurosci. 10:1407–1414.
Leone DP, Srinivasan K, Chen B, Alcamo E, McConnell SK. 2008. The determination of projection neuron identity in the developing cerebral cortex. Curr Opin Neurobiol. 18:28–35.
Madisen L, Zwingman TA, Sunkin SM, Oh SW, Zariwala HA, Gu H, Ng LL, Palmiter RD, Hawrylycz MJ, Jones AR et al. 2010. A robust and high-throughput Cre reporting and characterization system for the whole mouse brain. Nat Neurosci. 13:133–140.
Mason A, Larkman A. 1990. Correlations between morphology and electrophysiology of pyramidal neurons in slices of rat visual cortex. II. Electrophysiology. J Neurosci. 10:1415–1428.
McKenna WL, Betancourt J, Larkin KA, Abrams B, Guo C, Rubenstein JL, Chen B. 2011. Tbr1 and Fezf2 regulate alternate corticofugal neuronal identities during neocortical development. J Neurosci. 31:549–564.
Mitchell BD, Macklis JD. 2005. Large-scale maintenance of dual projections by callosal and frontal cortical projection neurons in adult mice. J Comp Neurol. 482:17–32.
Miyata T, Kawaguchi A, Okano H, Ogawa M. 2001. Asymmetric inheritance of radial glial fibers by cortical neurons. Neuron. 31:727–741.
Molyneaux BJ, Arlotta P, Hirata T, Hibi M, Macklis JD. 2005. Fezl is required for the birth and specification of corticospinal motor neurons. Neuron. 47:817–831.
Molyneaux BJ, Arlotta P, Menezes JR, Macklis JD. 2007. Neuronal subtype specification in the cerebral cortex. Nat Rev Neurosci. 8:427–437.
Mori M, Kose A, Tsujino T, Tanaka C. 1990. Immunocytochemical localization of protein kinase C subspecies in the rat spinal cord: light and electron microscopic study. J Comp Neurol. 299:167–177.
Noctor SC, Flint AC, Weissman TA, Dammerman RS, Kriegstein AR. 2001. Neurons derived from radial glial cells establish radial units in neocortex. Nature. 409:714–720.
Nolan MF, Malleret G, Lee KH, Gibbs E, Dudman JT, Santoro B, Yin D, Thompson RF, Siegelbaum SA, Kandel ER et al. 2003. The hyperpolarization-activated HCN1 channel is important for motor learning and neuronal integration by cerebellar Purkinje cells. Cell. 115:551–564.
Rash BG, Richards LJ. 2001. A role for cingulate pioneering axons in the development of the corpus callosum. J Comp Neurol. 434:147–157.
Sessa A, Mao CA, Hadjantonakis AK, Klein WH, Broccoli V. 2008. Tbr2 directs conversion of radial glia into basal precursors and guides neuronal amplification by indirect neurogenesis in the developing neocortex. Neuron. 60:56–69.
Sheets PL, Suter BA, Kiritani T, Chan CS, Surmeier DJ, Shepherd GM. 2011. Corticospinal-specific HCN expression in mouse motor cortex: I(h)-dependent synaptic integration as a candidate microcircuit mechanism involved in motor control. J Neurophysiol. 106:2216–2231.
Shim S, Kwan KY, Li M, Lefebvre V, Sestan N. 2012. Cis-regulatory control of corticospinal system development and evolution. Nature. 486:74–79.
Soriano P. 1999. Generalized lacZ expression with the ROSA26 Cre reporter strain. Nat Genet. 21:70–71.
Srinivasan K, Leone DP, Bateson RK, Dobreva G, Kohwi Y, Kohwi-Shigematsu T, Grosschedl R, McConnell SK. 2012. A network of genetic repression and derepression specifies projection fates in the developing neocortex. Proc Natl Acad Sci U S A. 109:19071–19078.
Stafstrom CE, Schwindt PC, Flatman JA, Crill WE. 1984. Properties of subthreshold response and action potential recorded in layer V neurons from cat sensorimotor cortex in vitro. J Neurophysiol. 52:244–263.
Stoenica L, Wilkars W, Battefeld A, Stadler K, Bender R, Strauss U. 2013. HCN1 subunits contribute to the kinetics of I(h) in neonatal cortical plate neurons. Dev Neurobiol. 73:785–797.
Tarabykin V, Stoykova A, Usman N, Gruss P. 2001. Cortical upper layer neurons derive from the subventricular zone as indicated by Svet1 gene expression. Development. 128:1983–1993.
Zhang L, Song NN, Chen JY, Huang Y, Li H, Ding YQ. 2012. Satb2 is required for dendritic arborization and soma spacing in mouse cerebral cortex. Cereb Cortex. 22:1510–1519.
Zimmer C, Tiveron MC, Bodmer R, Cremer H. 2004. Dynamics of Cux2 expression suggests that an early pool of SVZ precursors is fated to become upper cortical layer neurons. Cereb Cortex. 14:1408–1420.